Possible Chemical Source of Discrepancy between in Vitro and in Vivo Tests in Nanotoxicology Caused by Strong Adsorption of Buffer Components

Possible Chemical Source of Discrepancy between in Vitro and in Vivo Tests in Nanotoxicology Caused by Strong Adsorption of Buffer Components

Arianna Marucco, Federico Catalano, Ivana Fenoglio, Francesco Turci, Gianmario Martra, and Bice Fubini

Department of Chemistry, Interdepartmental Centre “G. Scansetti” for Studies on Asbestos and Other Toxic Particulates, and Interdepartmental Center for Nanostructured Interfaces and Surfaces (NIS), University of Torino, Via P. Giuria 7, 10125 Torino, Italy

1 Introduction

In particle toxicology, and particularly in nanotoxicology, large variability is often reported in the results of different experimental studies concerning the potential pathogenicity of the same material. This is ascribed, on the one hand, to the use of materials having the same chemical composition but different particle or surface morphology(1, 2) and, on the other hand, to differences in the employed cellular models or experimental designs.

Understandably, comparison between in vivo and in vitro tests often show even more marked discrepancies due to the great difference between the two kinds of experiments.(3, 4) However, there is an urgent need for in vitro screening assays to evaluate nanoparticle (NP) toxicity; thus, the reasons for discrepancies/consistency should be unveiled.(5)

Different buffering agents can be used to control the stability of the physiological pH during in vitro experiments among which the most common ones are PBS (a mixture of monohydrogen- and dihydrogen phosphate having physiological osmolarity) and HEPES, the organic molecule 4-(2-hydroxyethyl)-1-piperazineethanesulfonic acid. This latter is the most common buffering agent employed in cellular experiments, also used to complement cell culture media such as Dulbecco's modified Eagle's medium (DMEM).(6)

Despite the equivalent functional behavior, these two buffering agents are significantly different in chemical nature. Thus, they might exhibit different behaviors when interacting with the nanoparticle surface and possibly sticking to it. In turn, this may influence the fate of the adsorption at the nanoparticle surface of other species present in the incubation media, typically proteins, through the formation of the so-called "protein corona," which in some cases constitutes the actual surface "seen" by cells.(7)

The crucial role played by the buffer composition in protein adsorption has been recognized since the development of chromatographic protein separation.(8-10) More recently, the effect of buffer on protein adsorption at the solid/liquid interface has been investigated on flat surfaces such as TiO_2 films(11, 12) and those of germanium and crystalline silica present in ATR/FTIR cells and quartz microbalance, respectively.(13, 14) Focusing on nanoparticles, phosphate species in PBS were recognized to play a detrimental role against the antioxidant activity of CeO_2 NPs toward DNA,(15) while silver NPs grown in HEPES buffer exerted cytoprotective activity toward HIV-1 infected cells.(16) Both effects might be partly related to the interaction of the buffer with the particle surface.

In the frame of a systematic study of the interaction of proteins with oxide nanoparticles,(17-19) here we report the results of a comparative investigation of the role played by the two common buffers PBS or HEPES in the adsorption of bovine serum albumin (BSA) on TiO_2 nanoparticles, which suggest a new possible source of discrepancies among different studies unrelated to structural differences among

particles but to the interaction with the particle surface of chemical species present in body fluids or in growth cell media.

Data concern a widely studied nano-TiO_2 powder, P25 Evonik (formerly Degussa), which is a mixture of anatase and rutile, often found to be one of the most cytotoxic(20, 21) among titania specimens.

Typically, in TiO_2 P25 rutile primary particles (ca. 40 nm in size(22)) account for ca. 7% of the specific surface area, while the overall surface behavior is dominated by anatase particles (ca. 25 nm in size(22)) exhibiting a truncated bipyramid-like shape, mainly enclosed by {101} facets.(23) Noticeably, on such surfaces water is adsorbed molecularly, whereas the dissociation in surface hydroxyl groups occurs on surface terminations exposing sites with a higher coordinative degree of unsaturation.(24)

2 Materials and Methods

2.1 TiO_2 Nanoparticles

Pyrogenic Aeroxide P25 anatase/rutile (ca. 80/20 wt %) powder was purchased from Evonik (Germany). The material exhibited a specific surface area, measured with the BET method (hereafter SSA_{BET}), of ca. 55 m^2/g.(23)

2.2 Reagents

Fatty acid free BSA, chosen as a model for human albumin, was purchased from Sigma-Aldrich and used without further purification. In all experiments, ultrapure Milli Q (Millipore) water was used. All other reagents were from Sigma-Aldrich.

2.3 ζ-Potential

ζ-potential was measured by means of electrophoretic light scattering (ELS) (ZetasizerNano-ZS, Malvern Instruments). For these measurements, TiO_2 particles were suspended in ultrapure water, 10 mM phosphate buffer (PBS), or HEPES and then sonicated for 2 min with a probe sonicator (100 W, 60 kHz, Sonoplus). The ζ-potential at different pH (2–9) values was measured before and after incubation with BSA by disrupting the buffers by adding acid (HCl 0.1 M) or base (NaOH 0.1 M).

2.4 X-ray Fluorescence (XRF)

The amount of phosphate ions and HEPES molecules adsorbed on the surface of TiO_2 nanoparticles was determined as follows: two samples were prepared, each in duplicate, by suspending 25 mg of powder in 5 mL of buffer (PBS or HEPES). Samples were then manually rotated end-over-end for 15 min and centrifuged. The resulting pellets were washed three times with ultrapure water in order to remove reversible and nonadsorbed species. Samples were then pelletized and analyzed by a μ-XRF Eagle III-XPL spectrometer equipped with an EDS Si(Li) detector and with an Edax Vision32 microanalytical system. A microfocus X-ray tube (80 × 80 μm), Rh anode (50 kV, 1 mA), air cooled was used to collect X-ray maps of the samples. The mean profile, resulting from 18 measurements collected

for each sample in 6 different areas, was obtained and the analyte/Ti ratio calculated in % atoms. These data were used as input for the calculations of phosphate ions/HEPES molecules per nm^2 of TiO_2 surface and as % of Ti^{4+} sites exposed on TiO_2 anatase {101} facets (Table 1).

2.5 **Albumin Adsorption Isotherms**

The amount of adsorbed proteins was determined as follows: 50 mg of TiO_2 P25 powder was suspended in 2.5 mL of buffered solutions and then added to 2.5 mL of buffered solution of BSA, in order to attain a final protein concentration ranging from 0.5 to 10 mg/mL. The resulting suspensions were stirred in a thermostatic stirrer at 37 °C for 1 h and centrifuged at 11.000 rpm, then filtered through a membrane filter (cellulose acetate, pore diameter 0.45 μm), and the concentration of protein in the supernatant was determined spectrophotometrically (λ_{abs} = 562 nm) by using the bicinchoninic acid assay. The amount of protein adsorbed on the particles was calculated by the decrease of their concentration in the supernatant after incubation. The results are reported as the mean value of at least three separate determinations ± standard error.

3 Results and Discussion

3.1 **Influence of Buffer Type on Surface Charge**

The surface charge assumed by a particle in a suspension may be estimated by measuring the ζ-potential. The ζ-potential variation as a function of pH is currently used for nanoparticle characterization.(25) These curves are deeply modified following the adsorption of molecules and can be used to assess the irreversibility of adsorption and relevant surface modifications.(25-30) The change in ζ-potential as a function of pH is of much interest in toxicology, one reason being the different pH values possibly experienced by the inhaled particles, e.g., from passing from the extracellular medium (7.4) into the phagolysosome (4.5), following internalization, e.g., by alveolar macrophages.

Figure 1 reports the ζ-potential of TiO_2 P25 particles suspended in water at room temperature and sonicated for 2 min (a, red curve). The surface charge progressively varies from negative at basic pH values to positive at acidic pH values with a point of zero charge (PZC) close to neutral pH. When the same measurements are repeated in HEPES (b, blue) or in the phosphate buffered saline suspension (c, black), both buffers lower the ζ-potential value at physiological pH from ca. −10 to ca. −30 mV. The curves remarkably differ both from each other and the one obtained in water. PZC is close to 5 with HEPES and ca. 2 with PBS. This indicated strong and different interactions of the buffer molecules with the particle surface.

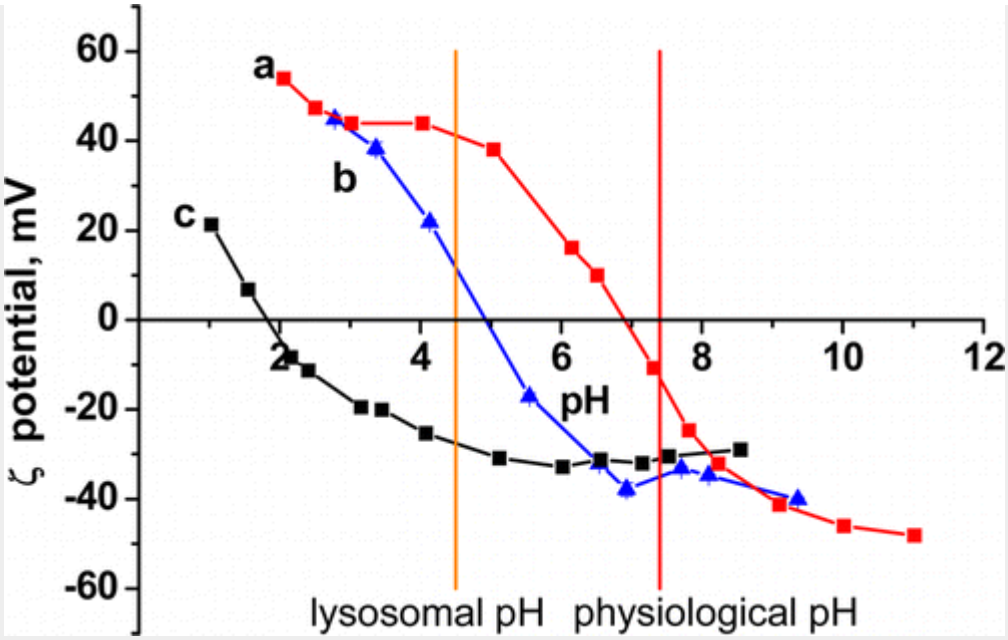

Figure 1. ζ-Potential of TiO_2 P25 as a function of the pH of the suspension in (a) water; (b) HEPES; and (c) PBS.

On such basis, aliquots of TiO_2 powder were incubated in the two buffers and washed in order to remove reversible and nonadsorbed species, and the amount of phosphate groups and HEPES molecules irreversibly adsorbed at the particle surface was measured by XRF. The results are reported in Table 1.

Table 1. Results of the XRF Measurement of the Amounts of Phosphates (Element Dosed: P) and HEPES (Element Dosed: S) Irreversibly Adsorbed on TiO_2 P25 in the Same Incubation Conditions as Those for BSA Adsorption

incubation analyte		analyte/Ti (atomic ratio)	analyte/TiO_2 (g/g)	phosphate/HEPES surface density (molecules/nm^2)[a]	phosphate/HEPES per Ti^{4+} sites on anatase TiO_2{101} facets (%)[b]
PBS/TiO_2	P	1.4×10^{-2}	5.4×10^{-3}	1.9	35
HEPES/TiO_2	S	6.7×10^{-5}	2.7×10^{-4}	9×10^{-2}	1.7

a

Calculated on the basis of SSA_{BET} = 55 m^2/g.

b

Calculated on the basis of 5.5 Ti^{4+} sites/nm^2 on TiO_2 anatase {101} facets.(23)

In both cases, the buffer species were found to be present at the surface of TiO_2 nanoparticles, but interestingly, the amount of HEPES irreversibly adsorbed was ca. 20 times lower with respect to phosphate anions. The anatase particles, which account for ca. 93% of the surface of TiO_2 P25, mainly expose {101} facets exhibiting a density of Ti^{4+} sites of ca. 5.5 atom/nm^2.(23) The data obtained therefore indicate that phosphate groups and HEPES molecules should occupy ca. 35 and 1.7%, respectively, of such surface cationic centers. Moreover, taking into account that HEPES molecules are significantly larger than phosphate groups and that each HEPES molecule might occupy at maximum a surface of ca. 0.3 nm^2, by assuming a side-on adsorption,(31) the percentage of surface Ti^{4+} sites occupied by HEPES molecules should increase at ca. 3%, still remaining 1 order of magnitude lower than what was found for phosphates.

The observed differences in ζ-potential may have important consequences: in fact, since the stability of a colloid depends upon the surface charge,(32) a different ζ-potential may lead to differences in terms of agglomerates size, thus probably yielding dissimilar toxicological effects elicited at the same virtual particle concentration. It is worth noting that at pH 4.5, the phagolysosome pH value, with PBS as the particle surface, will be negatively charged, whereas with HEPES a positive surface charge will be present, which also may account for different toxicological outcomes.

3.2 **Influence of Buffer on Adsorption of Bovine Serum Albumin**

The adsorption of bovine serum albumin (BSA) is described in Figure 2. The results are expressed as the amount of protein adsorbed on TiO_2 vs BSA concentration of the solution, buffered with either PBS or HEPES, in which NPs were incubated (panel A) and as a function of the amount of the free protein in the supernatant following incubation (panel B). Both representations show that the curves corresponding to the two buffers remarkably differ from one another, in that adsorption is about 5-fold higher with HEPES than with PBS at subphysiological BSA concentration (physiological 50g/L). The curves in panel A evidence that the presence of PBS remarkably reduces BSA uptake. In panel B, it is shown that in the presence of HEPES, but not of PBS, most of the BSA adsorption takes place without leaving free BSA in solution even at the lowest initial concentrations. However, in both cases, some BSA is still present in the solution at the highest concentration, thus excluding any limiting effect due to protein consumption.

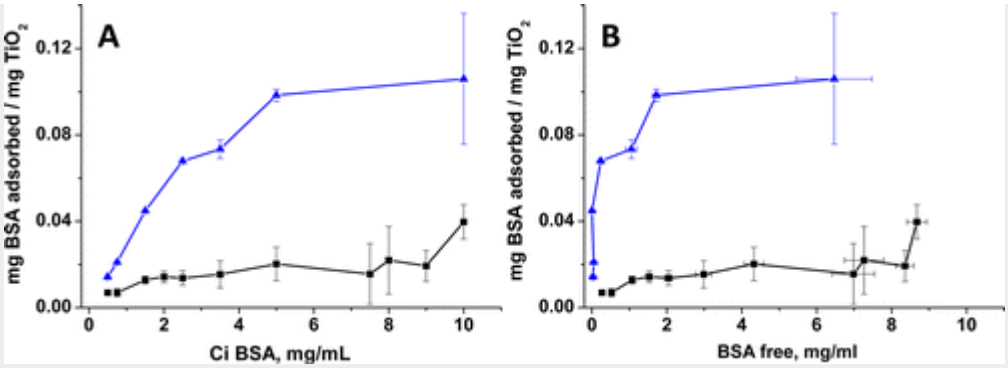

Figure 2. Adsorption of BSA on TiO_2 P25 nanoparticles in HEPES (blue triangles), and in PBS (black squares). Amount of protein adsorbed per mg of TiO_2 vs BSA initial concentration (panel A) and vs BSA final (equilibrium) concentration in the incubation media (panel B).

These differences are likely due to the interaction of phosphate ions with the titania surface. Inorganic phosphate ions are in fact known to strongly interact with TiO_2 surfaces,(33) the sites for phosphate adsorption being Lewis acid sites, i.e., Ti^{4+} ions exposed on {101} surfaces.(34) Water molecules coordinated to such Lewis acid centers could be displaced by incoming phosphates. The irreversible occupation of Ti^{4+} Lewis acidic sites where BSA may be adsorbed as well as electrostatic repulsions between negative charges may account for such a different adsorption behavior. The data herein well agrees with evidence for the detrimental role of phosphate species toward the adsorption on TiO_2 films of BSA(11) and immunoglobulin G.(12)

3.3**Changes in ζ-Potential- pH Curves Caused by BSA Adsorption**

Upon adsorption of BSA, the ζ-potential vs pH curve is expected to be modified because the surface is progressively covered by albumin. This has allowed us to gain information on the protein coverage attained and/or the occurrence of irreversible modifications of adsorbed proteins.(18) In the case of TiO_2 P25, it must be considered that surface hydroxyl groups, primarily responsible for the surface potential on the basis of their pH depending on the protonation/deprotonation status, are present only on a minor part of the NP surface and not homogeneously distributed on it: as reported above, TiO_2 NP are mainly limited by {101} facets that are hydrated and not hydroxylated. Anyway, the information provided by these measurements is meaningful. Figure 3 reports the ζ-potential vs pH curves measured after adsorption on TiO_2 of increasing amounts of BSA in both buffers up to the final concentrations shown in Figure 2.

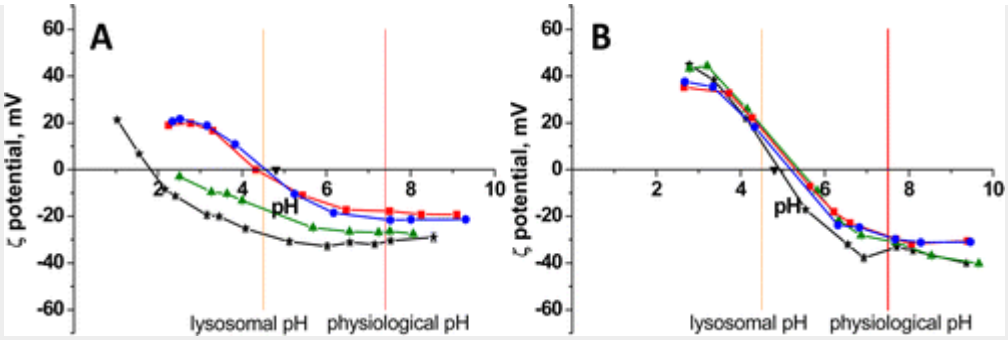

Figure 3. Variation of ζ-potential after albumin adsorption. Upon increasing concentration in the suspension, the point of zero charge (PZC) of TiO_2 shifts toward the isoelectric point (pI) of albumin. The curves are relative to TiO_2 P25 before (black stars) and after incubation with different albumin concentrations: 10 (red squares), 5 (blue circles), and 0.5 g/L (green triangles) in PBS (A) and HEPES (B).

With PBS, the presence of adsorbed BSA shifts the curves to the right and brings the PZC close to the isoelectric point (pI) of the protein, whereas with HEPES no remarkable changes are observed. These observed differences between HEPES and PBS were expected since TiO_2 P25 nanoparticles in the presence of HEPES have a PZC close to the pI of BSA, whereas this is not the case in the presence of PBS.

Interestingly, even at the highest concentrations employed, the curves obtained with the two buffers differ one from the other. In particular at lysosomal pH the ζ-potential value is always positive when HEPES is employed, whereas with PBS it is negative at low concentration and close to PZC upon increasing concentration.

To evidence the irreversibility of protein adsorption, albumin contacted titania were subjected to three centrifugation/redispersion cycles in ultrapure water in order to remove the nonadsorbed species, and the ζ-potential was measured as a function of pH. The curves did not change significantly at any coverage (not reported), suggesting a substantial irreversibility of protein adsorption in the case of phosphate buffer.

A similar procedure was used to evidence the irreversible surface modifications produced by mere contact with the buffer (as reported in Figure 4). Clearly, the surface properties are irreversibly modified following adsorption of both buffers, but the modification caused by PBS is much more pronounced than that caused by HEPES. This may account for the observed differences in protein uptake (Figure 2).

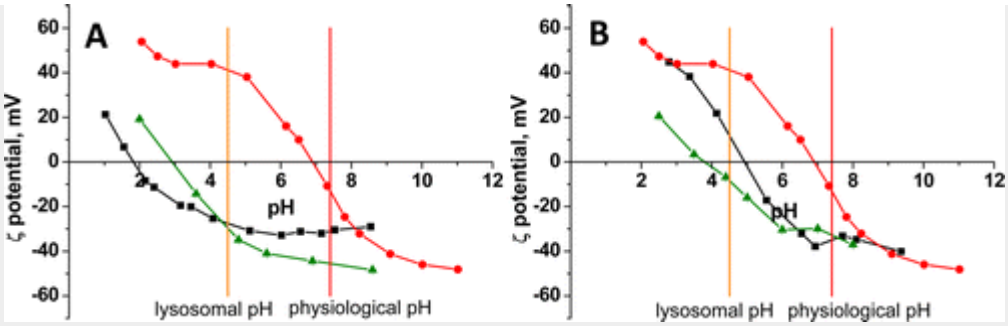

Figure 4. Surface modifications caused by buffers. In order to remove the nonadsorbed species (after contact with both PBS and HEPES), the nanoparticles onto which the buffers were adsorbed were subjected to three centrifugation/redispersion cycles in ultrapure water, and the ζ-potential was measured as a function of pH. Panel A, NP in water (red circles), PBS (black squares), and in water after contact with PBS (green triangles). Panel B, NP in water (red circles), HEPES (black squares), and in water after contact with HEPES (green triangles).

The results highlight the importance of the choice of buffer in toxicological studies. In fact, adsorbed proteins at the NP surface were reported to interfere with cell uptake,(35, 36) while the specific binding of protein affects particle biodistribution in vivo.(37, 38) The level of serum, where albumin is a major component, was reported to modulate cellular response,(39) namely, proliferation and genotoxicity, in A549 human lung cells exposed to various nanomaterials.(40) A protective effect of plasma toward the silica nanoparticle-induced hemolysis and cytotoxicity(41) was assigned to the protein layer shielding the surface.

4 Conclusions

The data reported herein indicate that the type of buffer used in toxicological tests may lead to different properties of the particle surface, with regard to features quite relevant to toxicity mechanisms, such as surface charge at relevant pH values, PZC, uptake, and modification of proteins. We suggest therefore that when investigating discrepancies between in vivo and in vitro tests performed on the same material, besides the most relevant features, e.g., related to the administration route, the surface modifications induced at the particle surface by natural vs artificial fluids should also be considered.

†Author Contributions

A.M. and F.C. contributed equally to this work.

References

1. Warheit, D. B., Webb, T. R., Reed, K. L., Frerichs, S., and Sayes, C. M. (2007) Pulmonary toxicity study in rats with three forms of ultrafine-TiO2 particles: Differential responses related to surface properties Toxicology 230, 90– 104

2. Fubini, B., Ghiazza, M., and Fenoglio, I. (2010) Physico-chemical features of engineered nanoparticles relevant to their toxicity Nanotoxicology 4, 347– 363

3. Sayes, C. M., Reed, K. L., and Warheit, D. B. (2007) Assessing toxicity of fine and nanoparticles: Comparing in vitro measurements to in vivo pulmonary toxicity profiles Toxicol. Sci. 97, 163– 180.

4. Schrurs, F. and Lison, D. (2012) Focusing the research effort Nat. Nanotechnol. 7, 546– 548.

5. Han, X., Corson, N., Wade-Mercer, P., Gelein, R., Jiang, J., Sahu, M., Biswas, P., Finkelstein, J. N., Elder, A., and Oberdoerster, G. (2012) Assessing the relevance of in vitro studies in nanotoxicology by examining correlations between in vitro and in vivo data Toxicology 297, 1– 9.

6. Eagle, H. (1971) Buffer combinations for mammalian cell culture Science 174, 500– 503.

7. Kasemo, B. (2002) Biological surface science Surf. Sci. 500, 656– 677

8. Bock, H. G., Skene, P., Fleischer, S., Cassidy, P., and Harshman, S. (1976) Protein purification: adsorption chromatography on controlled pore glass with the use of chaotropic buffers Science 191, 380– 383.

9. Fornstedt, N., Fornstedt, T., and Porath, J. (1993) Influence of buffer composition on protein adsorption on agarose (sepharose-6B) Chromatographia 35, 387– 389.

10. van Sommeren, A. P. G., Machielsen, P. A. G. M., and Gribnau, T. C. J. (1992) Effects of temperature, flow-rate and composition of binding buffer on adsorption of mouse monoclonal IgG1 antibodies to protein - a sepharose-4 fast flow Prep. Biochem. 22, 135– 149.

11. do Serro, P. V. A., Fernandes, A. C., Saramago, B. D. V., and Norde, W. (1999) Bovine serum albumin adsorption on titania surfaces and its relation to wettability aspects J. Biomed. Mater. Res. 46, 376– 381.

12. Moulton, S. E., Barisci, J. N., McQuillan, A. J., and Wallace, G. G. (2003) ATR-IR spectroscopic studies of the influence of phosphate buffer on adsorption of immunoglobulin G to TiO2 Colloids Surf., A 220, 159– 167.

13. Wei, T., Kaewtathip, S., and Shing, K. (2009) Buffer effect on protein adsorption at liquid/solid interface J. Phys. Chem. C 113, 2053– 2062.

14. Parkes, M., Myant, C., Cann, P. M., and Wong, J. S. S. (2014) The effect of buffer solution choice on protein adsorption and lubrication Tribol. Int. 72, 108– 117.

15. Xue, Y., Zhai, Y., Zhou, K., Wang, L., Tan, H., Luan, Q., and Yao, X. (2012) The vital role of buffer anions in the antioxidant activity of CeO2 nanoparticles Chem.—Eur. J. 18, 11115– 11122.

16. Sun, R. W. Y., Chen, R., Chung, N. P. Y., Ho, C. M., Lin, C. L. S., and Che, C. M. (2005) Silver nanoparticles fabricated in Hepes buffer exhibit cytoprotective activities toward HIV-1 infected cells Chem. Commun. 40, 5059– 5061.

17. Marucco, A., Fenoglio, I., Turci, F., and Fubini, B. (2013) Interaction of fibrinogen and albumin with titanium dioxide nanoparticles of different crystalline phases. J. Phys.: Conf. Ser. 429, DOI: , DOI: 10.1088/1742-6596/429/1/012014 .

18. Marucco, A., Turci, F., O'Neill, L., Byrne, H. J., Fubini, F., and Fenoglio, I. (2014) Hydroxyl density affects the interaction of fibrinogen with silica nanoparticles at physiological concentration J. Colloid Interface Sci. 419, 86– 94.

19. Marucco, A., Gazzano, E., Ghigo, D., Enrico, E., and Fenoglio, I. (2014) Fibrinogen enhances the inflammatory response of alveolar macrophages to TiO2, SiO2 and carbon nanomaterials Nanotoxicology, DOI: 10.3109/17435390.2014.978405.

20. Sayes, C. M., Wahi, R., Kurian, P. A., Liu, Y. P., West, J. L., Ausman, K. D., Warheit, D. B., and Colvin, V. L. (2006) Correlating nanoscale titania structure with toxicity: A cytotoxicity and inflammatory response study with human dermal fibroblasts and human lung epithelial cells Toxicol. Sci. 92, 174– 185.

21. Gerloff, K., Fenoglio, I., Carella, E., Kolling, J., Albrecht, C., Boots, A. W., Forster, I., and Schins, R. P. F. (2012) Distinctive toxicity of TiO2 rutile/anatase mixed phase nanoparticles on Caco-2 cells Chem. Res. Toxicol. 25, 646– 655.

22. Mino, L., Spoto, G., Bordiga, S., and Zecchina, A. (2012) Particles morphology and surface properties as investigated by HRTEM, FTIR, and periodic DFT calculations: from pyrogenic TiO2 (P25) to nanoanatase J. Phys. Chem. C 11, 17008– 17018.

23. Deiana, C., Minella, M., Tabacchi, G., Maurino, V., Fois, E., and Martra, G. (2013) Shape-controlled TiO2 nanoparticles and TiO2 P25 interacting with CO and H2O2 molecular probes: a synergic approach for surface structure recognition and physico-chemical understanding Phys. Chem. Chem. Phys. 15, 307– 315.

24. Deiana, C., Fois, E., Coluccia, S., and Martra, G. (2010) Surface structure of TiO2 P25 nanoparticles: Infrared study of hydroxy groups on coordinative defect sites J. Phys. Chem. C 114, 21531– 21538.

25. Mahmoudi, M., Lynch, I., Ejtehadi, M. R., Monopoli, M. P., Bombelli, F. B., and Laurent, S. (2011) Protein-nanoparticle interactions: Opportunities and challenges Chem. Rev. 111, 5610– 5637.

26. Rezwan, K., Studart, A. R., Voros, J., and Gauckler, L. J. (2005) Change of ζ potential of biocompatible colloidal oxide particles upon adsorption of bovine serum albumin and lysozyme J. Phys. Chem. B 109, 14469– 14474.

27. Lundqvist, M., Stigler, J., Elia, G., Lynch, I., Cedervall, T., and Dawson, K. A. (2008) Nanoparticle size and surface properties determine the protein corona with possible implications for biological impacts Proc. Natl. Acad. Sci. U.S.A. 105, 14265– 14270.

28. Berg, J. M., Romoser, A., Banerjee, N., Zebda, R., and Sayes, C. M. (2009) The relationship between pH and zeta potential of similar to 30 nm metal oxide nanoparticle suspensions relevant to in vitro toxicological evaluations Nanotoxicology 3, 276– 283.

29. Fenoglio, I., Fubini, B., Ghibaudi, E. M., and Turci, F. (2011) Multiple aspects of the interaction of biomacromolecules with inorganic surfaces Adv. Drug Delivery Rev. 63, 1186– 1209.

30. Mura, S., Hillaireau, H., Nicolas, J., Le Droumaguet, B., Gueutin, C., Zanna, S., Tsapis, N., and Fattal, E. (2011) Influence of surface charge on the potential toxicity of PLGA nanoparticles towards Calu-3 cells Int. J. Nanomed. 6, 2591– 2605.

31. Wouters, J., Haming, L., and Sheldrick, G. (1996) HEPES Acta Crystallogr., Sect. C 52, 1687– 1688.

32. Israelachvili, J. (1992) Intermolecular and Surface Forces, 2nd ed., p 213, Academic Press, London.

33. Ikeguchi, Y. and Nakamura, H. (1997) Determination of organic phosphates by column-switching high performance anion-exchange chromatography using on-line preconcentration on titania Anal. Sci. 13, 479– 483.

34. Hadjiivanov, K. I., Klissurski, D. G., and Davydov, A. A. (1989) Study of phosphate-modified TiO2 (anatase) J. Catal. 116, 498– 505.

35. Oberdorster, G. (2010) Safety assessment for nanotechnology and nanomedicine: concepts of nanotoxicology J. Int. Med. 267, 89– 105.

36. Monopoli, M. P., Walczyk, D., Campbell, A., Elia, G., Lynch, I., Bombelli, F. B., and Dawson, K. A. (2011) Physical-chemical aspects of protein corona: Relevance to in vitro and in vivo biological impacts of nanoparticles J. Am. Chem. Soc. 133, 2525– 2534.

37. Ehrenberg, M. S., Friedman, A. E., Finkelstein, J. N., Oberdoerster, G., and McGrath, J. L. (2009) The influence of protein adsorption on nanoparticle association with cultured endothelial cells Biomaterials 30, 603– 610.

38. Dobrovolskaia, M. A., Aggarwal, P., Hall, J. B., and McNeil, S. E. (2008) Preclinical studies to understand nanoparticle interaction with the immune system and its potential effects on nanoparticle biodistribution Mol. Pharmaceutics 5, 487– 495.

39. Gonzalez, L., Sanderson, B. J. S., and Kirsch-Volders, M. (2011) Adaptations of the in vitro MN assay for the genotoxicity assessment of nanomaterials Mutagenesis 26, 185– 191.

40. Corradi, S., Gonzalez, L., Thomassen, L. C. J., Bilanicova, D., Birkedal, R. K., Pojana, G., Marcomini, A., Jensen, K. A., Leyns, L., and Kirsch-Volders, M. (2012) Influence of serum on in situ proliferation and genotoxicity in A549 human lung cells exposed to nanomaterials Mutat. Res., Genet. Toxicol. Environ. Mutagen. 745, 21– 27.

41. Shi, J., Hedberg, Y., Lundin, M., Wallinder, I. O., Karlsson, H. L., and Möller, L. (2012) Hemolytic properties of synthetic nano- and porous silica particles: The effect of the surface properties and the protection by the plasma corona Acta Biomater. 8, 3478– 3490.